Using Metabolic Theory to Describe Temperature and Thermal Acclimation Effects on Parasitic Infection

Jason P. Sckrabulis,[1,*] Karie A. Altman,[2] and Thomas R. Raffel[1]

1. Department of Biological Sciences, Oakland University, Rochester, Michigan 48309; 2. Department of Biology, St. Bonaventure University, St. Bonaventure, New York 14778

Submitted June 27, 2021; Accepted January 5, 2022; Electronically published April 18, 2022

Online enhancements: supplemental PDF. *Dryad data:* https://doi.org/10.5061/dryad.bnzs7h4c7.

abstract: Predicting temperature effects on species interactions can be challenging, especially for parasitism, where it is difficult to experimentally separate host and parasite thermal performance curves. Prior authors proposed a possible solution based on the metabolic theory of ecology (MTE), using MTE-based equations to describe the thermal mismatch between host and parasite performance curves and account for thermal acclimation responses. Here, we use published infection data, supplemented with experiments measuring metabolic responses to temperature in each species, to show that this modeling framework can successfully describe thermal acclimation effects on two different stages of infection in a tadpole-trematode system. All thermal acclimation effects on host performance manifested as changes in one key model parameter (activation energy), with measurements of host respiration generating similar MTE parameter estimates and acclimation effects compared with measurements of the host's ability to clear encysted parasites. This result suggests that metabolic parameter estimates for whole-body metabolism can sometimes be used to estimate temperature effects on host and parasite performance curves. However, we found different thermal patterns for measurements of host prevention of initial parasite encystment emphasizing potential challenges when applying MTE-based models to complex parasite-host systems with multiple distinct stages of infection.

Keywords: host-parasite interactions, thermal performance curve, *Ribeiroia ondatrae*, *Lithobates clamitans*.

Introduction

The threat of climate change makes it increasingly important to understand how temperature influences species interactions, such as predation and parasitism (Studer and Poulin 2013; Dell et al. 2014; Luhring and DeLong 2016; Rohr and Cohen 2020). Temperature can have complex effects on species interactions because the outcome of the interaction (e.g., parasite infection) depends on the thermal responses of both participants (e.g., host and parasite; Thomas and Blanfield 2003; Raffel et al. 2013; Cohen et al. 2017; Rohr et al. 2018). However, most current mathematical models of how temperature influences parasitism focus only on the thermal responses of one organism at a time (host or parasite). Furthermore, both nonlinear and thermal acclimation responses to temperature can have important effects on parasitism, particularly in fluctuating-temperature environments (Shi and Ge 2010; Rohr et al. 2013; Molnár et al. 2017). However, these responses are seldom incorporated into models predicting parasite-host responses to climate, in part because of the difficulty of developing and parameterizing equations to describe such a complex set of interacting factors. How hosts and parasites respond to temperature variation is vital to understanding the overall effects of climate change on infectious diseases (Raffel et al. 2013; Rohr and Cohen 2020).

The metabolic theory of ecology (MTE) offers potential solutions for modeling the complex thermal biology of species interactions, including parasitism (Molnár et al. 2013, 2017; Kirk et al. 2018). Based on first principles of chemistry and physics, MTE postulates that metabolism is a fundamental rate underlying ecological processes that scales predictably with temperature and body size (Gillooly et al. 2001, 2016; Brown et al. 2004). In the MTE framework, models describing the temperature dependence of biological processes (e.g., physiological performance curves) are typically derived from the Arrhenius equation for enzyme reaction rates (Arrhenius 1889; Brown et al. 2004). Such models benefit from being naturally curvilinear and composed of biologically meaningful parameters, which can have broadly similar values among disparate taxa or different physiological processes. For example, the activation energy for metabolism (E_a) usually falls between 0.2

* Corresponding author; email: jason.sckrabulis@gmail.com.

ORCIDs: Sckrabulis, https://orcid.org/0000-0002-6901-094X; Altman, https://orcid.org/0000-0003-2595-3767; Raffel, https://orcid.org/0000-0003-2525-0834.

and 1.2 eV for species ranging from unicellular organisms to plants and vertebrates (Gillooly et al. 2001; Brown et al. 2004; Dell et al. 2011).

Furthermore, metabolic performance curves can be derived from a variety of physiological processes, such as oxygen consumption and muscle power, and different metabolic proxies can often provide similar estimates for key model parameters like E_a (Dell et al. 2011). This apparent generalizability among physiological processes within an organism might make it possible to estimate key model parameters for species interactions, by independently measuring metabolic proxies for the performance of each species (Rohr et al. 2013; Molnár et al. 2017). This could be especially helpful for modeling parasitic infection because the most direct metrics of organism performance—parasite infectivity and host resistance—are typically quantified using a response variable that represents a single outcome resulting from these two processes (e.g., prevalence or intensity of infection) rather than a direct measure of either organism's performance (Molnár et al. 2017). MTE-based models provide a promising solution for resolving separability problems that can arise when trying to parameterize separate host and parasite thermal performance curves based on available infection data (Molnár et al. 2017). This approach provides the opportunity to simultaneously investigate the temperature dependence of each organism's thermal performance curve in the context of an active infection, potentially providing insights into biological mechanisms driving the thermal biology of host susceptibility to parasitism. Additionally, this approach may reveal easily measured metabolic proxies for parasite infectivity or host resistance, potentially enabling researchers to predict the responses of multiple host species to a single parasite, including for endangered species, where infection experiments may be impossible to conduct.

Molnár et al. (2013) showed that MTE-based models can be used to model the temperature-dependent developmental rate of a parasite's free-living environmental stage. Rohr et al. (2013) proposed an extension of this approach to describe the temperature dependence of parasitic infection as the difference (i.e., "mismatch") between two rate processes represented by separate thermal performance curves, one describing parasite infectivity i_T and the other describing host resistance to infection r_T. Rohr et al. (2013) defined infectivity as the instantaneous rate of increase (i.e., exponential growth rate parameter) for a parasite in or on a host, in the absence of host resistance. However, our study focused on two stages of macroparasitic infection, neither of which involves direct multiplication of the parasite within its host (Anderson and May 1979). For our model, we instead defined infectivity i_T as the geometric rate of change in the parasite population over a discrete time step ($\lambda_T = N_{t+1}/N_t$; Gotelli 2008), in the absence of host resistance. Because of the lack of within-host parasite replication, i_T was constrained to be between 0 and 1—that is, $i_T = 1 - d_T$, where d_T is the discrete rate of background parasite mortality and i_T is the discrete rate of parasite survival over a single time step in the absence of host resistance. Host resistance to infection r_T is then defined as the host's ability to decrease parasite survival over the same time step (i.e., $\lambda_T = 1 - d_T - r_T = i_T - r_T$). Infectivity and resistance are modeled as separate functions of temperature using an MTE-based model of thermal performance (see "MTE-Based Thermal Performance Curves"). This modeling framework is consistent with the thermal mismatch hypothesis of Cohen et al. (2017, 2019), which postulates that the temperature dependence of infection depends on the difference (or mismatch) between the parasite and host thermal performance curves (for examples, see fig. S1; figs. S1–S6 are available online). However, because of the exponential nature of MTE-based thermal performance curves, the shape of a curve resulting from this mismatch (i.e., the temperature dependence of parasite population growth or survival on a host) will not necessarily be well described by a single MTE-based performance curve, as illustrated in figure S1.

Thermal acclimation effects—that is, changes in hosts or parasite performance curves following extended exposure to warm or cool temperatures—are also important to understand and predict climate effects on infectious disease (Raffel et al. 2013). Thermal acclimation effects can be incorporated into the proposed modeling framework by making key metabolic parameters functions of acclimation temperature (Gillooly et al. 2006; Rohr et al. 2013). For example, an activation energy that increases as a function of acclimation temperature can be used to describe a type of beneficial acclimation response, where an organism has increased performance at its acclimation temperature relative to organisms acclimated to other temperatures (Wilson and Franklin 2002; Altman et al. 2016). A scaling constant that increases or decreases with acclimation temperature can be used to describe a "warmer is better" or "cooler is better" response, respectively, where organisms acclimated to warmer or cooler temperatures have elevated performance across the full range of temperatures (Wilson and Franklin 2002; Altman et al. 2016). Curvilinear effects of acclimation temperature on activation energy or the scaling constant can be used to describe scenarios when performance is greatest at an intermediate temperature, consistent with an optimum temperature response (Wilson and Franklin 2002). Which model parameters change in response to thermal acclimation may have implications for our understanding of the mechanisms driving acclimation responses; for example, changes in activation energy might reflect altered expression of rate-limiting enzymes, whereas a decreased scaling constant might reflect an overall

decrease in host energy reserves (the thermal stress hypothesis; Paull et al. 2015). Note that this same general approach could be used to incorporate other variables that might affect parasite or host performance; for example, dose-dependent host resistance could be incorporated by making the scaling constant a function of the infectious dose (Johnson et al. 2012; Calhoun et al. 2019).

Here, we show that this modeling framework can successfully describe temperature dependence of and thermal acclimation effects on *Ribeiroia ondatrae* infection in its green frog tadpole intermediate host, *Lithobates* [*Rana*] *clamitans*, using data generated by Altman et al. (2016). *Rana ondatrae* is a snail-borne trematode parasite that uses *Helisoma* [*Planorbella*] *trivolvis* as a first intermediate host and tadpoles as a second intermediate host (Johnson et al. 2004). From the parasite's perspective, infection of tadpoles is a multistage process, where (1) the free-swimming *R. ondatrae* cercaria stage must find and encyst in the tadpole (i.e., parasite encystment) and (2) the encysted *R. ondatrae* metacercaria must persist within the tadpole until the host is consumed by a definitive host (i.e., cyst survival). From the host's perspective, the tadpole resists infection by (1) reducing the probability of a parasite penetrating and encysting (i.e., prevention of encystment) and (2) clearing encysted metacercariae from its body via the immune response (i.e., cyst clearance). The data set generated by Altman et al. (2016) is unique because they quantified rates of cercaria penetration, encystment as metacercaria, and survival within tadpoles through time, allowing us to distinguish between the encystment and cyst survival stages of infection. To investigate whether other aspects of physiological performance can serve as reasonable metabolic proxies for parasite infectivity or host resistance in an MTE-based model, we supplemented this data set with two new experiments, one quantifying the temperature dependence of *R. ondatrae* cercaria swimming speed and one quantifying the temperature dependence of respiration in uninfected tadpoles. We then used model fitting to determine whether the difference between the MTE-based curves for infectivity and resistance reasonably describes the temperature dependence of parasite survival at each stage of infection. Metacercariae are thought to have limited metabolic activity once encysted (but see Cwiklinski et al. 2018), so we made the simplifying assumption that metacercaria "infectivity" during the cyst survival stage would be constant in the absence of host resistance (i.e., 100% survival, or $i_T = 1$). This means that the temperature dependence of metacercaria clearance should be almost entirely driven by variation in host resistance, providing us with a unique opportunity to conduct a more direct test of the MTE-based modeling approach for host resistance than would be possible in other systems. Comparing the metacercaria clearance results with tadpole respiration allowed us to test the hypothesis that some MTE parameters are generalizable across physiological processes within a single host species. We show that this framework can be used to describe linear and curvilinear effects of acclimation temperature on host resistance and that metabolic proxies such as cercaria swimming speed and host respiration generated reasonable estimates of key MTE parameters for models describing parasite infectivity and host resistance to infection.

Methods

MTE-Based Thermal Performance Curves:

The simplest MTE-based models are those derived from the original Arrhenius equation, such as the Boltzmann-Arrhenius (BA) formulation:

$$\mathrm{BA}(T) = P_{T_0} \exp\left(-\left(\frac{E_a}{k}\right)\left(\frac{1}{T} - \frac{1}{T_0}\right)\right), \quad (1)$$

where P_{T_0} is the performance at standardization temperature T_0, k is Boltzmann's constant ($k = 8.62 \times 10^{-5}$ eV K^{-1}), and E_a is the activation energy. However, the BA model assumes that performance increases exponentially with temperature and may be unable to describe physiological processes at extreme high or low temperatures, particularly when a data set extends above the temperature for peak performance, in which case the BA model may generate unreasonable activation energy estimates (Molnár et al. 2017). The more complex Sharpe-Schoolfield (SS) model includes additional parameters describing reversible enzyme deactivation at extreme high or low temperatures (Schoolfield et al. 1981). Here, we utilize a SS model modification that accounts only for the decrease at extreme high temperatures (i.e., modification of the SS model for high-temperature deactivation; Molnár et al. 2017):

$$\mathrm{SS}(T) = \mathrm{BA}(T) \times \left[1 + \exp\left(\left(\frac{E_d^H}{k}\right)\left(\frac{1}{T_d^H} - \frac{1}{T}\right)\right)\right]^{-1}, \quad (2)$$

where T_d^H is the high temperature for deactivation and E_d^H is the deactivation energy. $\mathrm{SS}(T)$ becomes approximately equal to $\mathrm{BA}(T)$ if the high temperature for deactivation (T_d^H) is much higher than the measured temperature range, in which case the right side of the equation approaches 1.0. Note that we use E_a, T_d^H, and E_d^H to refer to the general MTE model parameters (e.g., eqq. [1], [2]), but we use other subscripts to identify parameters for specific processes (see table 1 for a full list of parameter definitions).

In our analysis, we considered both the BA model and the SS model as a potential candidate for describing thermal performance for each process. We expected that the rate processes measured in this study and by Altman et al. (2016) would exhibit declines if measured at sufficiently high

Table 1: Full list of parameter definitions for the modeling framework (eqq. [1], [2]), including acclimation effect functions used in model fitting and analysis (eqq. [3]–[5])

Parameter	Definition	Unit
i_{T_0}, r_{T_0}, c_{T_0}, R_{T_0}	Parasite infectivity i, host resistance r, cyst clearance c, and respiration R constant at standardization temperature $T_{0(i,r,c,R)}$	…
E_i, E_r, E_c, E_R	Activation energies of infectivity, resistance, clearance, and respiration processes	eV
E_i^H, E_r^H, E_c^H, E_R^H	Deactivation energy for infectivity, resistance, clearance, and respiration at high (H) temperature	eV
T_i^H, T_r^H, T_c^H, T_R^H	High temperature of deactivation for infectivity, resistance, clearance, and respiration processes	°C[a]
k	Boltzmann's constant	eV K^{-1}
C	Translation constant to allow for a lower threshold for infectivity	…[b]
$\varepsilon.X$	Intercept terms of the acclimation effect on X, where X is the parameter in question	…
$\beta.X$	Linear terms of the acclimation effect on X, where X is the parameter in question	…
$\alpha.X$	Quadratic terms of the acclimation effect on X, where X is the parameter in question	…

[a] Temperatures are presented in degrees Celsius for clarity; however, their use in the model requires transformation into kelvins by adding 273.15.
[b] C has units equivalent to the proportion of metacercaria encysted.

temperatures, requiring use of the SS model to describe these processes. However, we preferred to use the simpler BA model when it resulted in a better model fit, indicating that the available data did not include sufficiently high temperatures to detect high-temperature deactivation. In some cases, we also incorporated upper or lower thresholds for performance, as described in later sections. The final performance curve model formulation for each physiological process is presented in table 2.

Sources of Experimental Data

To test whether this modeling framework can successfully describe effects of temperature and thermal acclimation on parasitic infection, we used data collected by Altman et al. (2016) on the effects of temperature and host thermal acclimation on *Rana ondatrae* encystment and cyst survival in *Lithobates clamitans* (data are available in the Dryad Digital Repository; Altman et al. 2017). In brief, tadpoles were acclimated to one of six "acclimation temperatures" and then shifted to one of six "performance temperatures" immediately prior to *R. ondatrae* exposure. All infected snails were acclimated to the performance temperature prior to cercaria collection, so that only the tadpole hosts experienced shifts in temperature; therefore, acclimation effects were not caused by parasite acclimation. Each tadpole was exposed to 20 fluorescently labeled cercariae (LaFonte and Johnson 2013) and imaged at 0.5, 7, and 14 days after exposure to determine the proportion of successfully encysted cercariae (at 0.5 days) and metacercaria (cyst) survival (at 7 and 14 days). Although the original data set quantified cyst survival at two time points, here we consider cyst survival only over the first week after infection (7 days) because Altman et al. (2016) did not detect significant acclimation effects in their analysis of the 14-day time point. We simplified statistical model fitting by setting a discrete time step of $\Delta t = 1$ for each stage of infection, where $t = 1$ is defined as 0.5 days for the encystment stage and 7 days for the metacercaria-survival stage. Detailed methods for this experiment are available in Altman et al. (2016).

We also conducted two new experiments to measure the temperature dependence of separate metabolic proxies for parasite infectivity (*R. ondatrae* cercaria swimming speed) and host resistance (*L. clamitans* oxygen consumption). Detailed methods are provided in the supplemental PDF, available online. All animal husbandry and experimental manipulations in this study were conducted in compliance with Oakland University Institutional Animal Care and Use Committee protocol 12111.

Statistical Methods: Fitting MTE-Based Models to Data

MTE-based models were fit to empirical data with R statistical software (R Core Team 2020) using nonlinear least squares optimization (nls function). The error distribution for thermal performance data is often lognormal, as a result of normally distributed biological parameters that appear in the exponential terms of SS models (Régnière and Powell 2003; Xiao et al. 2011; Régnière et al. 2012; Molnár et al. 2017). However, empirical performance data can also be normally distributed (Xiao et al. 2011). For each biological response variable, we used Xiao et al.'s (2011) methods to calculate comparable Akaike information criterion (AIC) values for models with normal versus lognormal error distributions. We also used AIC to determine whether the more complicated SS model (adding deactivation energy E_d^H and high temperature for deactivation T_d^H as free parameters) was a better fit than the BA model. Our statistical code and data can be found in the Dryad Digital Repository (https://doi.org/10.5061/dryad.bnzs7h4c7; Sckrabulis et al. 2022).

In typical MTE-based models of thermal performance, the standardization temperature (T_0) is an arbitrarily selected

Table 2: Final model formulation for each quantified aspect of parasite or host performance

Response, model component	Parsimonious model characteristics	Equation
Cercaria velocity (experiment 1):		
Parasite infectivity metabolic proxy	Sharpe-Schoolfield,[a] lognormal residuals	$i_T = i_{T_0} \exp\left(-\left(\frac{E_i}{k}\right)\left(\frac{1}{T} - \frac{1}{T_{0_i}}\right)\right) \cdot \left[1 + \exp\left(\left(\frac{E_i^H}{k}\right)\left(\frac{1}{T_i^H} - \frac{1}{T}\right)\right)\right]^{-1}$
Tadpole respiration (experiment 2):		
Host resistance metabolic proxy	Sharpe-Schoolfield,[a] normal residuals	$R_T = R_{T_0} \exp\left(-\left(\frac{E_R}{k}\right)\left(\frac{1}{T} - \frac{1}{T_{0_R}}\right)\right) \cdot \left[1 + \exp\left(\left(\frac{E_R^H}{k}\right)\left(\frac{1}{T_R^H} - \frac{1}{T}\right)\right)\right]^{-1}$
Parasite encystment (Altman et al. 2016):		
Parasite infectivity (encystment)	Sharpe-Schoolfield,[a] normal residuals, C allows for a parasite performance level below which encystment is 0%	$i_T = i_{T_0} \exp\left(-\left(\frac{E_i}{k}\right)\left(\frac{1}{T} - \frac{1}{T_{0_i}}\right)\right) \cdot \left[1 + \exp\left(\left(\frac{E_i^H}{k}\right)\left(\frac{1}{T_i^H} - \frac{1}{T}\right)\right)\right]^{-1} - C$
Host resistance (prevent encystment)	Boltzmann-Arrhenius, normal residuals	$r_T = r_{T_0} \exp\left(-\left(\frac{E_r}{k}\right)\left(\frac{1}{T} - \frac{1}{T_{0_r}}\right)\right)$
Parasite survival (Altman et al. 2016):		
Parasite infectivity (cyst survival)	Assumed 100% survival in the absence of host resistance	$i_T = 1$
Host resistance (clear parasites)	Sharpe-Schoolfield,[a] normal residuals	$c_T = c_{T_0} \exp\left(-\left(\frac{E_c}{k}\right)\left(\frac{1}{T} - \frac{1}{T_{0_c}}\right)\right) \cdot \left[1 + \exp\left(\left(\frac{E_c^H}{k}\right)\left(\frac{1}{T_c^H} - \frac{1}{T}\right)\right)\right]^{-1}$

[a] Modified Sharpe-Schoolfield model that incorporates high-temperature deactivation but not low-temperature deactivation.

temperature that can be interpreted as the temperature where performance equals the scaling constant P_{T_0} in the absence of enzyme deactivation (Schoolfield et al. 1981; Molnár et al. 2013). However, in models where we allowed activation energy E_a to vary as a function of acclimation temperature, T_0 became a meaningful parameter because it formed the inflection point where performance curves from all acclimation treatments were constrained to cross (fig. S2). See the supplemental PDF for a detailed explanation of this problem and how we optimized T_0 in models that incorporated thermal acclimation.

Statistical Methods: Single-Species Performance Curves (Cercaria Velocity and Tadpole Respiration)

We fit models to the cercaria swimming speed data as a proxy for infectivity i_T to obtain estimates for infectivity at standardization temperature i_{T_0} and activation energy for infectivity E_i. This model did not include acclimation effects on metabolic parameters (i.e., all snails and parasites were acclimated to the same temperature), making the choice of the standardization temperature for infectivity T_{0_i} arbitrary (Molnár et al. 2013); therefore, we selected a T_{0_i} value within the lower range of experimental performance temperatures ($T_{0_i} = 19$°C).

We modeled the metabolic performance curve for uninfected tadpoles using the mass-specific respiration rate data. To avoid confusion between parameters, we used R for host respiration in place of r host resistance. We initially fit models without acclimation effects (as described above for cercaria swimming speed) for tadpole respiration rate R_T to obtain reasonable initial starting values for respiration at the standardization temperature R_{T_0}, activation energy for respiration E_R, the deactivation energy for respiration at high temperatures E_R^H, and the high temperature for deactivation for respiration T_R^H. To incorporate host thermal acclimation effects into the model, we made each parameter into a quadratic function of acclimation temperature as follows:

$$R_{T_0} = \varepsilon.R_{T_0} + \beta.R_{T_0} \times T_{\text{Accl}} + \alpha.R_{T_0} \times T_{\text{Accl}}^2, \quad (3)$$

$$E_R = \varepsilon.E_R + \beta.E_R \times T_{\text{Accl}} + \alpha.E_R \times T_{\text{Accl}}^2, \quad (4)$$

$$T_R^H = \varepsilon.T_R^H + \beta.T_R^H \times T_{\text{Accl}} + \alpha.T_R^H \times T_{\text{Accl}}^2, \quad (5)$$

where the ε terms are intercept parameters, the β terms are linear coefficient parameters, and the α terms are quadratic coefficient parameters. According to the principle of marginality, any model with a quadratic term (α) always included its corresponding linear term (β). Acclimation temperatures were centered around zero to facilitate model convergence and to allow interpretation of linear terms in models containing polynomial terms. The standardization temperature for respiration rate T_{0_R} estimate was manually optimized through a set of values around the range of temperature data were collected in models where acclimation effects on E_R were present ($T_{0_R} = 14.55$°C; fig. S3*A*). SS models converged readily when E_R^H was optimized as a free parameter.

Statistical Methods: Parasite Encystment in Tadpoles

We used metabolic parameter estimates for the activation energy for infectivity E_i, the deactivation energy for infectivity E_i^H, and the high temperature of deactivation energy for infectivity T_i^H from the best-fit cercaria swimming speed model to partially parameterize a system of equations describing the proportion of cercariae that encysted as metacercariae in their tadpole hosts, based on the hypothesized thermal mismatch between the parasite and host thermal performance curves. Because of challenges with parameterizing an implied host resistance curve (for the prevention of encystment) without direct data, we used the port algorithm in nls, which is more robust than the default Gauss-Newton for obtaining model convergence with bounded parameter estimates. We initially estimated a new value for infectivity at standardization temperature i_{T_0} (which is dependent on the scale of the response variable) for the infectivity curve and the resistance at standardization temperature r_{T_0} and activation energy for resistance E_r for the entire data set without any thermal acclimation effects to obtain better starting parameters for future, more complex models. We also incorporated an upper threshold into the infectivity equation because i_T cannot be greater than 1.0 for proportion data, which we achieved by using conditional programming within the model. Biologically, this threshold represents a swimming speed above which cercariae are fully capable of infecting a host ($i_T = 1$), and because *R. ondatrae* cercaria swim nearly constantly throughout their life span (Beaver 1939), we felt justified in making this assumption. Likewise, we compared this model fit to a model where we added a lower threshold where infectivity cannot be less than zero, achieved by adding a translation constant C to the model to enable the curve to cross into negative values (where $C > 0$) and restricting infectivity to $i_T = 0$ in those cases using conditional programming within the model (table 2). The model with both an upper and a lower threshold on infectivity had a better fit (AIC $= -152.876$) than a model with only an upper threshold (AIC $= -127.362$) and a model with no thresholds (AIC $= -100.93$).

To investigate thermal acclimation effects on major metabolic parameters for host resistance (r_{T_0}, E_r, T_r^H), we made these parameters into linear functions of acclimation temperature (i.e., we removed quadratic coefficients from eqq. (3)–(5) by setting $\alpha = 0$ and substituted resistance r in place of respiration R). Acclimation temperatures

were centered around zero, to facilitate model convergence. We conducted ranked AIC comparisons considering all combinations of linear change in these parameters, and we manually optimized the standardization temperature for respiration T_{0_r} in any model with an acclimation effect on E_r ($T_{0_r} = 19$°C; fig. S3*B*). The model with the best statistical fit by AIC value was then subjected to backward model selection to potentially remove any nonsignificant parameters based on *P* values to determine a final model.

Statistical Methods: Metacercaria (Cyst) Survival and Metabolic Parameter Comparison

We assumed that all metacercaria would have survived in the absence of host resistance (i.e., no parasite background mortality; $d_T = 0$), such that $i_T = 1$. Therefore, we were able to simplify the modeling of the interaction between parasite infectivity (cyst survival) and host resistance (cyst clearance) by treating the system as a single-species host process (as described above for cercaria swimming speed and tadpole respiration). It is important to note that fully modeling the mismatch as proportion survived (i.e., the inverse of proportion cleared) as the difference between constant infectivity ($i_T = 1$) and metacercaria clearance instead would yield the same result, and we present the full thermal mismatch model for a more direct comparison to the parasite encystment stage of infection. To differentiate the parameters for clearance from those used in the proportion of parasites encysted model above, we substituted *c* in models describing metacercaria clearance by the tadpole (table 2). We fit a model without acclimation effects for host clearance of metacercaria c_T to obtain reasonable initial starting values for clearance at standardization temperature c_{T_0}, activation energy for clearance E_c, and deactivation energy and high temperature for deactivation for clearance E_c^H and T_c^H, respectively. Altman et al. (2016) found a significant quadratic effect of acclimation temperature on metacercaria survival in this data set; therefore, we sought to determine which MTE model parameters (c_{T_0}, E_c, or T_c^H) could best account for this curvilinear acclimation effect by replacing respiration *R* in equations (3)–(5) with *c*, describing acclimation effects on cyst clearance. All combinations of linear and quadratic effects on model parameters were considered during model selection, and we manually optimized the standardization temperature T_{0_c} in any model with an acclimation effect on E_c ($T_{0_c} = 26.9$°C; fig. S3*C*). When we allowed E_c^H to vary as a free parameter in the SS model, we were unable to achieve model convergence. We therefore followed the approach of Molnár et al. (2013) where $E_a \ll E^H$ (i.e., $5 \times E_a = E^H$), we fixed E_c^H at 3.25 eV, based on the overall average activation energy across organisms of 0.65 eV (Gillooly et al. 2001; Brown et al. 2004). After model selection, we confirmed that this assumption was justified for this data set based on the average E_c (i.e., $E_c^H \approx 5 \times 0.64\ \text{eV} = 3.21\ \text{eV}$) across all acclimation temperatures.

To test the assumption of MTE that metabolic parameters are generalizable across processes within the same species, we generated bootstrapped 95% confidence bands around the quadratic acclimation effect of the best-fit models for metacercaria clearance and uninfected host respiration. We also optimized a model fit to the clearance rate data where the quadratic acclimation temperature effect on E_c was equal to that of the estimates for E_R obtained from the uninfected tadpole respiration rate model. We fixed T_{0_R} equal to the original value from the metacercaria clearance rate equation to compare model predictions more directly, and we optimized only c_{T_0}, which again is dependent on the scale of the response variable.

Results

The best-fit model to describe *Ribeiroia ondatrae* cercariae swimming speed was an SS model assuming lognormal error (fig. S4; tables 2, S1 [tables S1–S8 are available online]; activation energy of infectivity $E_i = 0.41 \pm 0.05$ eV; high temperature of deactivation of infectivity $T_i^H = 31.59$°C $\pm$ 0.66°C). All plus-or-minus errors reported in text represent 95% confidence intervals. All final model formulations and parsimonious characteristics can be found in table 2.

For the proportion-encysted data set, the best model describing acclimation effects used a BA-based equation for host prevention of encystment with normal error while allowing the activation energy for host prevention E_r to vary linearly with the tadpole's acclimation temperature (AIC $= -164.084$; fig. 1; tables 2, 3, S1; $\beta = 0.036 \pm 0.024$; $\varepsilon = 0.41 \pm 0.17$). The linear effect of acclimation temperature on E_r is consistent with statistical results presented in the original empirical study, which found a statistical interaction between the effects of acclimation temperature and performance temperature (Altman et al. 2016). Allowing other model parameters to vary with acclimation temperature did not result in further improvements to model AIC (table S2). Our model projects that cercariae swimming slower than 1.7 mm/s were unable to infect tadpoles ($i_T = 0$ below 6.8°C and above 34.3°C), and cercariae swimming faster than 3.1 mm/s had maximum infection potential ($i_T = 1$ between 16.7°C and 32.1°C) in the absence of host defenses.

For the metacercaria (cyst) survival data set, the best model describing acclimation effects was an SS model for cyst clearance by the host with normal error, which also allowed the activation energy for cyst clearance E_c to vary as a curvilinear function of acclimation temperature (AIC $= 88.965$; tables 2, 3, S3; $\alpha = 0.015 \pm 0.006$;

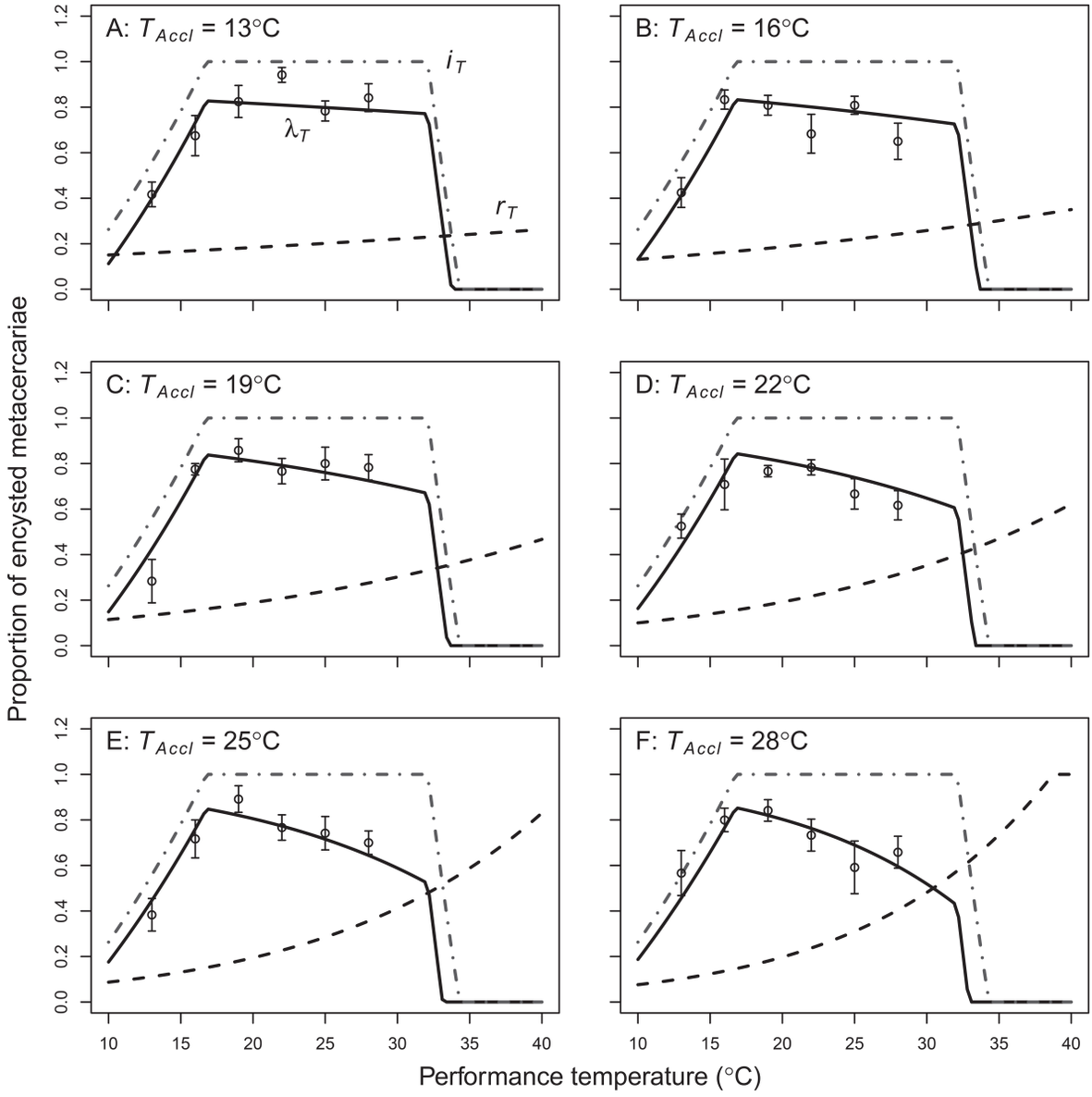

Figure 1: Thermal mismatch model describing acclimation effects on the encystment stage of parasite infection in tadpoles. The model describes a linear change in the activation energy for host resistance (E_r) as a function of acclimation temperature (T_{Accl}), with greater model-estimated E_r values (steeper slopes) occurring at higher acclimation temperatures (13°C: $E_r = 0.142$ eV; 16°C: $E_r = 0.249$ eV; 19°C: $E_r = 0.358$ eV; 22°C: $E_r = 0.466$ eV; 25°C: $E_r = 0.574$ eV; 28°C: $E_r = 0.682$ eV). Each panel represents the model fit to data from one acclimation temperature. In each panel, the dotted-dashed line shows the model-estimated thermal performance curve for parasite infectivity (i.e., parasite encystment in the absence of host resistance: i_T), the dashed curve represents the model-estimated thermal performance curve for host resistance to encystment (r_T), and the solid curve shows the resulting model prediction for the temperature-dependent rate of parasite encystment (λ_T). Open circles represent the mean proportion at each performance temperature (bars show standard errors).

$\beta = -0.017 \pm 0.026; \varepsilon = 0.261 \pm 0.217$). This model accounted for both the shape of the performance-temperature effect on metacercaria clearance and the curvilinear effect of tadpole acclimation reported by Atman et al. (2016; see fig. 2). Making other MTE parameters into functions of acclimation temperature did not result in improved model AIC (table S4). For tadpole respiration, the best model describing acclimation effects was also an SS model, allowing the activation energy for respiration E_R to vary as a curvilinear function of acclimation (AIC = −2,275.59; fig. 3*A*;

Table 3: Final model ANOVA of acclimation temperature effects on the activation energies from the final selected thermal models for various aspects of host performance

Model, parameter	*F*	df	*P*
Proportion encysted:			
$\beta.E_r$	9.2766	1, 213	.002614
Metacercaria clearance:			
$\alpha.E_c$	31.996	1, 207	<.0005
$\beta.E_c$	1.7153	1, 208	.1917
Tadpole respiration:			
$\alpha.E_R$	16.523	1, 205	<.0005
$\beta.E_R$	3.2814	1, 206	.0715

Note: See table 1 for parameter definitions. The models presented here have linear (β) or quadratic (α) terms for describing thermal acclimation effects on activation energy for their respective host process. Quadratic effects always abided by marginality and included the linear term.

tables 2, 3, S5; $\alpha = 0.002 \pm 0.001$; $\beta = 0.00002 \pm 0.004$; $\varepsilon = 0.607 \pm 1.18$). Allowing other MTE parameters to vary with acclimation temperature did not result in further improvements to model AIC (table S6).

To directly compare mean values of key MTE parameters for different metrics of host performance (resisting or preventing encystment, cyst clearance, and respiration rate), we reran each of the best-fit models with acclimation effects removed. For the proportion-encysted data set, the best model describing the overall effects of performance temperature assumed normal error, used a BA equation for host resistance, and included a lower cercaria velocity threshold below which infectivity equaled zero ($E_r = 0.44 \pm 0.27$ eV). For the cyst survival data set, the best model describing overall effects of performance temperature on cyst clearance by the host was an SS model assuming normal error ($E_c = 0.55 \pm 0.25$ eV; $T_c^H = 31.84°C \pm 5.06°C$). For tadpole respiration, the best model describing overall effects of performance temperature was also an SS model with normal error ($E_R = 0.69 \pm 0.22$ eV; $T_R^H = 35.05°C \pm 1.78°C$).

Discussion

These analyses show that MTE-based models can be used to successfully describe complex effects of temperature on trematode infection in tadpoles by describing each stage of infection (i.e., parasite encystment and cyst survival) as the thermal mismatch between parasite and host thermal performance curves. Furthermore, we show that thermal acclimation effects on host resistance to infection can be described within an MTE modeling framework by incorporating linear or curvilinear effects of thermal acclimation on key metabolic parameters (tables S1, S3, S5). Acclimation effects on both stages of infection were best described by allowing the host activation energy, E_a, to vary as a function of acclimation temperature. Interestingly, tadpole clearance of encysted parasites showed similar patterns of temperature dependence to whole-body tadpole respiration (fig. 3*C*), with overlapping confidence intervals for the values of key MTE parameters, the high temperature for deactivation T_d^H, and E_a, as well as a curvilinear effect of thermal acclimation on E_a. This result suggests a link between a tadpole's metabolic rate and its ability to clear encysted parasites, as predicted by MTE. In contrast, tadpole resistance to parasite encystment generated a lower mean E_a value that increased as a function of host acclimation temperature. This result implies that tadpole prevention of parasite encystment is at least partially decoupled from the temperature dependence of whole-body metabolism.

The findings for host clearance of encysted parasites lend credence to a core postulate of MTE, namely, that physiological and ecological rate processes are fundamentally limited by organism metabolic rates (Gillooly et al. 2001; Brown et al. 2004). This postulate underlies a core assumption of the MTE-based modeling approach used in this study: that physiological processes underlying organism performance (e.g., immune responses underlying host resistance responses) will have similar values for key model parameters compared with those derived from whole-body metabolism. To our knowledge, the current study provides the first experimental test of this assumption for host resistance to infection, which is usually difficult to experimentally or statistically separate from the temperature dependence of parasite infectivity. *Lithobates clamitans* clearance of *Ribeiroia ondatrae* metacercariae provides a unique opportunity to experimentally isolate effects of temperature on host resistance because the physiological dormancy of encysted metacercariae allows us to make the simplifying assumption that parasite infectivity (survival) is constant across the experimental temperatures. However, in half of the acclimation temperatures, parasite survival was lower at the coolest performance temperature 13°C (i.e., metacercaria clearance by the host

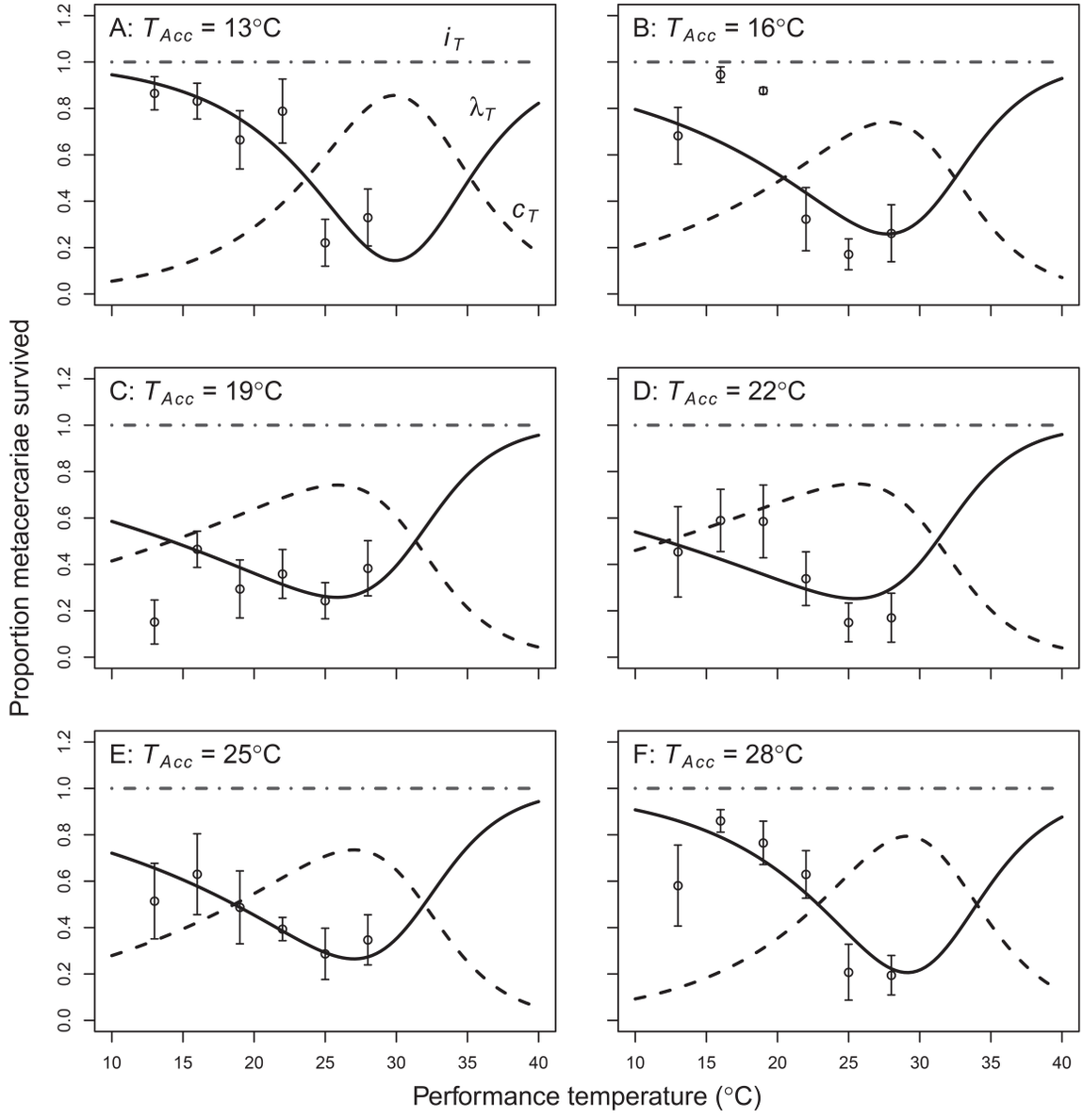

Figure 2: Thermal mismatch model describing acclimation effects on the cyst survival stage of parasite infection in tadpoles. The model describes a quadratic change in the activation energy for host resistance E_c as a function of acclimation temperature (T_{Accl}), with the greater model-estimated E_c values (steeper slopes) at higher or lower acclimation temperatures (13°C: $E_c = 1.203$ eV; 16°C: $E_c = 0.63$ eV; 19°C: $E_c = 0.318$ eV; 22°C: $E_c = 0.268$ eV; 25°C: $E_c = 0.48$ eV; 28°C: $E_c = 0.953$ eV). In each panel, the dotted-dashed horizontal line shows the assumed constant rate of parasite infectivity (i.e., cyst survival in the absence of host resistance: $i_T = 1$), the dashed curve represents the model-estimated thermal performance curve for cyst clearance (c_T), and the solid curve shows the resulting model prediction for the temperature-dependent rate of metacercaria survival (λ_T). Open circles represent the mean survival at each performance temperature (bars show standard errors).

was higher), suggesting a potential shortcoming in the modeling approach. Parasite encystment rates were lower overall at this performance temperature, possibly allowing for more complete clearance by the host immune response, which might help account for this pattern. Comparisons with measurements of whole-body tadpole respiration revealed quantitatively similar values for the key physiological parameters E_a and T_d^H. The high temperature for deactivation of host respiration was 35.0°C, and the high temperature for deactivation of cyst clearance was 31.23°C. The average activation energy for respiration across all acclimation temperatures was 0.66 eV, whereas

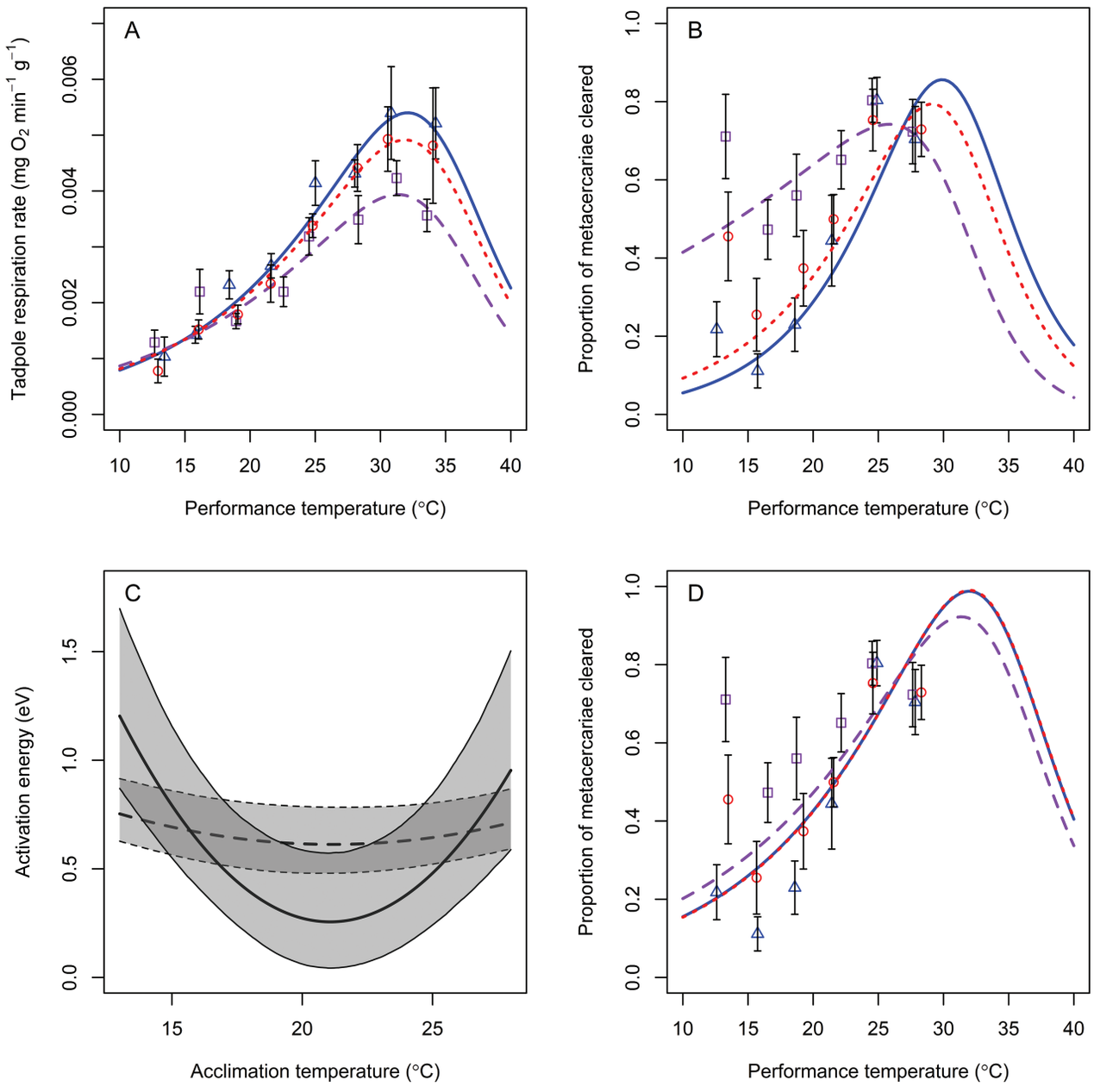

Figure 3: Comparison of thermal acclimation effects on the activation energies of uninfected host respiration and metacercariae clearance by the host. *A* depicts the best-fit model predictions for quadratic thermal acclimation effects on E_R for host respiration for three acclimation temperatures (13°C: solid blue, triangles; 22°C: dashed purple, squares; 28°C: dotted red, diamonds). *B* summarizes the best-fit model predictions for acclimation effects on E_c for cyst clearance for the same acclimation temperatures. However, acclimation temperature groups for the clearance data are grouped for clarity (low, blue: 13°C and 16°C; intermediate, purple: 19°C and 22°C; high, red: 25°C and 28°C). *C* shows the quadratic change in activation energy as a function of thermal acclimation temperature for both cyst clearance (solid) and uninfected tadpole respiration (dashed). Thick lines represent the quadratic effect described in table S4 (clearance) and table S6 (respiration). Thin lines and shaded areas show the 95% confidence interval. *D* depicts cyst clearance data identical to *B*; however, the model predictions are generated using parameter estimates from the best-fit model for tadpole respiration rather than from cyst clearance itself. Note that the high and low acclimation temperature curves nearly overlap and are difficult to distinguish. All points represent average values at each performance temperature (bars show standard error).

the average activation energy for cyst clearance was 0.64 eV, both of which are near the average activation energy value for all taxa (Brown et al. 2004). Additionally, host respiration and cyst clearance both yielded qualitatively similar curvilinear effects of acclimation temperature on activation energy (fig. 3*B*, 3*D*). These findings show that it is possible to use a relatively straightforward measurement of physiological performance, such as organism respiration, as a proxy to predict the temperature dependence of a host's ability to clear a parasitic infection.

Unlike our findings for metacercaria clearance, resistance to parasite encystment generated qualitatively different patterns of temperature dependence from tadpole respiration, suggesting that this component of host resistance is at least partially decoupled from host metabolic rate, consistent with studies that found different patterns of acclimation for different performance metrics (Wilson et al. 2000; McWhinnie et al. 2021). Why might some components of host resistance be less tightly linked to host metabolism than others? In the case of *R. ondatrae* infection in tadpoles, it seems clear that different aspects of the immune system are involved at different stages of infection. Relative to clearance of encysted parasites, the encystment process occurs on a much shorter timescale (minutes to hours instead of the days to weeks required for metacercaria clearance by a host; Rohr et al. 2008; Pochini and Hoverman 2017) and involves different host tissues (e.g., skin). We hypothesize that resistance to encystment may be less limited by host metabolic rate than clearance of metacercariae, because of the short timescale of this process and thus greater reliance on constitutive immune defenses. By "constitutive," we refer here to defense mechanisms that were produced and locally present prior to parasite exposure, such as peptides, complement, physical barriers, and locally available cells like macrophages (Mangoni et al. 2001; Rollins-Smith et al. 2002; Woodhams et al. 2007; Davis et al. 2008). In contrast, clearance of encysted parasites occurs on a timescale of days to weeks and is more likely to rely on processes limited by rates of cellular metabolism, such as migration of immune cells to the site of infection and production of new immune cells and/or proteins to attack the parasite (Patel et al. 2009; Gervasi et al. 2013). We postulate that host clearance mechanisms occurring on longer timescales and relying on inducible defenses (e.g., acquired immune responses) may be more limited by metabolic rate than constitutive defenses and thus more likely to be predictable using MTE-based modeling approaches. Further studies would be needed to test the potential generality of this hypothesis and whether it applies to other aspects of host performance, such as behavioral resistance mechanisms. For example, a tadpole's ability to dislodge an attached cercaria prior to skin penetration might depend on its metabolism-limited muscle performance, whereas its ability to select a relatively parasite-free microhabitat might be decoupled from metabolism (Taylor et al. 2004; Daly and Johnson 2011; Szuroczki and Richardson 2012). It would also be interesting to explore approaches like those used by Dell et al. (2014) or Öhlund et al. (2015) to predict attack rates based on predator and prey relative velocities. Some species of trematode larvae, such as *R. ondatrae*, swim constantly once released into the environment (Beaver 1939), which is partly analogous to active-capture predation and might be more predictive of initial infection rates.

Even though host prevention of parasite encystment had different patterns of temperature dependence from host respiration, it was nevertheless possible to describe the complex pattern of temperature-dependent parasite encystment using MTE-based thermal models. The parasite encystment model's fit was substantially improved by incorporating a lower threshold velocity (swimming speed) below which cercariae were unable to infect hosts ($i_T = 0$; fig. 1). This finding is consistent with empirical observations taken during the cercaria swimming speed experiment. At our two highest temperature treatments, most cercariae were unable to swim up into the water column (K. A. Altman, personal observation). Although parasite infectivity is a complex trait involving multiple physiological adaptations and host-seeking behaviors (Graczyk and Shiff 2000; Fingerut et al. 2003; Smith and Cohen 2012), our results suggest that cercaria velocity is a reasonable proxy for parasite infectivity for predicting the temperature dependence of *R. ondatrae* infections.

For all three metrics of host performance in this study, our analysis revealed that thermal acclimation effects were best described within an MTE-based modeling framework by allowing the activation energy parameter to vary as a function of acclimation temperature (figs. 1–3). These results may have implications for what types of physiological changes may drive observed effects of thermal acclimation on performance of *L. clamitans* tadpoles. Which physiological mechanisms drive acclimation effects on thermal performance curves remains an important outstanding question in thermal biology. Most of what we know about mechanistic drivers of thermal acclimation relates to expression of heat-shock proteins (HSP), which is likely more relevant for parameters describing tolerance of extreme high temperatures, such as CT_{max} (Tomanek and Somero 1999; Narum et al. 2013). Changes to the slope of the thermal performance curve following warm- or cold-temperature acclimation, as observed in this study, could be driven by changes in expression of rate-limiting metabolic enzymes or enzymes specific to immune function. Alternatively, the acclimation effects could be driven by changes in overall host body condition following exposure to stressful warm or cool temperatures (Geiser 2004;

Paull et al. 2015). Such "thermal stress" effects would be expected to reduce overall tadpole performance across all temperatures rather than changing the slope of the performance curve, unless there was some sort of additional constraint on host performance (e.g., upper limits for rates of respiration or cyst clearance at high temperatures; fig. 3).

Conclusions

Taken together, these experiments and models show that the MTE-based approach proposed by Rohr et al. (2013), which describes the temperature dependence of infection as the thermal mismatch between parasite and host performance curves, can be successfully applied to describe complex temperature and thermal acclimation effects on a model host-parasite system. We also show that thermal acclimation effects on various aspects of green frog performance can be described by making E_a a function of acclimation temperature, with potential implications for the physiological mechanisms underlying these acclimation effects. Furthermore, this study provides validation for a key assumption of MTE-based models to describe thermal performance, namely, that key parameters like E_a will have similar values across physiological processes within a species (Gillooly et al. 2001; Brown et al. 2004; Dell et al. 2011; Molnár et al. 2017). The potential for parameter generality across taxa and physiological systems makes MTE-based modeling a potentially powerful approach to describe the temperature dependence of parasitism, particularly for systems involving large numbers of potential host species that might not be amenable to direct infection experiments (e.g., trematode or fungal infections in threatened amphibian species). However, our results suggest that some aspects of parasite infectivity or host resistance are more closely tied to organism metabolic rates than others, so researchers should take caution in selecting metabolic proxies for parasite or host performance or making untested assumptions about parameter generality. Future studies should focus on determining whether and how different aspects of parasite infectivity and host resistance relate to organism metabolic rates, to assess the general utility of MTE-based thermal models for predicting temperature dependence of internal parasitism and other species interactions.

Acknowledgments

We thank the P. T. J. Johnson lab for providing feces from trematode-infected rats. We also thank Y. Ashaqua, J. Dunn, and E. L. Godfrey for their contributions to animal maintenance and video processing. J.P.S., K.A.A., and T.R.R. were supported by National Science Foundation grants to T.R.R. (CAREER: IOS-1651888 and IOS-1121529) and by Oakland University Graduate Provost Awards to K.A.A. and J.P.S.. K.A.A. was also supported by a King-Chávez-Parks Future Faculty Fellowship.

Statement of Authorship

J.P.S., K.A.A., and T.R.R. conceived and designed the study; K.A.A. conducted the cercaria swimming speed experiment; K.A.A. and J.P.S. conducted the tadpole respiration experiment; J.P.S. and T.R.R. developed the modeling approach and analyzed the data; J.P.S. wrote the manuscript; J.P.S., K.A.A., and T.R.R. reviewed and edited the manuscript; and J.P.S., K.A.A., and T.R.R. acquired the funding.

Data and Code Availability

Data from the cercaria swimming speed and uninfected green frog tadpole respiration experiments can be found in the Dryad Digital Repository (https://doi.org/10.5061/dryad.bnzs7h4c7; Sckrabulis et al. 2022). Example video files and statistical R code are also available on Zenodo (https://doi.org/10.5281/zenodo.5718847, https://doi.org/10.5281/zenodo.5722416).

Literature Cited

Altman, K. A., S. H. Paull, P. T. J. Johnson, M. N. Golembieski, J. P. Stephens, B. E. LaFonte, and T. R. Raffel. 2016. Host and parasite thermal acclimation responses depend on the stage of infection. Journal of Animal Ecology 85:1014–1024. https://doi.org/10.1111/1365-2656.12510.

———. 2017. Data from: Host and parasite thermal acclimation responses depend on the stage of infection. Journal of Animal Ecology 85:1014–1024, Dryad Digital Repository, https://doi.org/10.5061/dryad.f3k8p.

Anderson, R. M., and R. M. May. 1979. Population biology of infectious diseases: part I. Nature 280:361–367. https://doi.org/10.1038/280361a0.

Arrhenius, S. 1889. Uber die reaktionsgeschwindigkeit bei der inversion von rohrzucker durch sauren. Zeitschrift Fur Physik Chemique 4:226–248. https://doi.org/10.1515/zpch-1889-0416.

Beaver, P. C. 1939. The morphology and life history of *Psilostomum ondatrae* Price, 1931 (Trematoda: Psilostomidae). Journal of Parasitology 25:383–389. https://doi.org/10.2307/3272305.

Brown, J. H., J. F. Gillooly, A. P. Allen, V. M. Savage, and G. B. West. 2004. Toward a metabolic theory of ecology. Ecology 85:1771–1789. https://doi.org/10.1890/03-9000.

Calhoun, D. M., K. L. Leslie, T. J. Achatz, T. McDevitt-Galles, V. V. Tkach, and P. T. J. Johnson. 2019. Patterns of *Clinostomum marginatum* infection in fishes and amphibians: integration of field, genetic, and experimental approaches. Journal of Helminthology 94:e44. https://doi.org/10.1017/S0022149X18001244.

Cohen, J. M., T. A. McMahon, C. Ramsay, E. A. Roznik, E. L. Sauer, S. Bessler, D. J. Civitello, et al. 2019. Impacts of thermal mismatches on chytrid fungus *Batrachochytrium dendrobatidis* prevalence are

moderated by life stage, body size, elevation, and latitude. Ecology Letters 22:817–825. https://doi.org/10.1111/ele.13239.

Cohen, J. M., M. D. Venesky, E. L. Sauer, D. J. Civitello, T. A. McMahon, E. A. Roznik, and J. R. Rohr. 2017. The thermal mismatch hypothesis explains host susceptibility to an emerging infectious disease. Ecology Letters 20:184–193. https://doi.org/10.1111/ele.12720.

Cwiklinski, K., H. Jewhurst, P. McVeigh, T. Barbour, A. G. Maule, J. Tort, S. M. O'Neill, M. W. Robinson, S. Donnelly, and J. P. Dalton. 2018. Infection by the helminth parasite *Fasciola hepatica* requires rapid regulation of metabolic, virulence, and invasive factors to adjust to its mammalian host. Molecular and Cellular Proteomics 17:792–809. https://doi.org/10.1074/mcp.RA117.000445.

Daly, E. W., and P. T. J. Johnson. 2011. Beyond immunity: quantifying the effects of host anti-parasite behavior on parasite transmission. Oecologica 165:1043–1050. https://doi.org/10.1007/s00442-010-1778-y.

Davis, A. K., D. L. Maney, and J. C. Maerz. 2008. The use of leukocyte profiles to measure stress in vertebrates: a review for ecologists. Functional Ecology 22:760–772. https://doi.org/10.1111/j.1365-2435.2008.01467.x.

Dell, A. I., S. Pawar, and V. M. Savage. 2011. Systematic variation in the temperature dependence of physiological and ecological traits. Proceedings of the National Academy of Sciences of the USA 108:10591–10596. https://doi.org/10.1073/pnas.1015178108.

———. 2014. Temperature dependence of trophic interactions are driven by asymmetry of species responses and foraging strategy. Journal of Animal Ecology 83:70–84. https://doi.org/10.1111/1365-2656.12081.

Fingerut, J. T., C. A. Zimmer, and R. K. Zimmer. 2003. Larval swimming overpowers turbulent mixing and facilitates transmission of a marine parasite. Ecology 84:2502–2515. https://doi.org/10.1890/02-4035.

Geiser, F. 2004. Metabolic rate and body temperature reduction during hibernation and daily torpor. Annual Review of Physiology 66:239–274. https://doi.org/10.1146/annurev.physiol.66.032102.115105.

Gervasi, S. S., E. G. Hunt, M. Lowry, and A. R. Blaustein. 2013. Temporal patterns in immunity, infection load and disease susceptibility: understanding the drivers of host responses in the amphibian-chytrid fungus system. Functional Ecology 28:569–578. https://doi.org/10.1111/1365-2435.12194.

Gillooly, J. F., A. P. Allen, V. M. Savage, E. L. Charnov, G. B. West, and J. H. Brown. 2006. Response to Clarke and Fraser: effects of temperature on metabolic rate. Functional Ecology 20:400–404.

Gillooly, J. F., J. H. Brown, G. B. West, V. M. Savage, and E. L. Charnov. 2001. Effects on size and temperature on metabolic rate. Science 293:2248–2251. https://doi.org/10.1126/science.1061967.

Gillooly, J. F., J. P. Gomez, E. V. Mavrodiev, Y. Rong, and E. S. McLamore. 2016. Body mass scaling of passive oxygen diffusion in endotherms and ectotherms. Proceedings of the National Academy of Sciences of the USA 113:5340–5345. https://doi.org/10.1073/pnas.1519617113.

Gotelli, N. J. 2008. A primer of ecology. 4th ed. Sinauer, Sunderland, MA.

Graczyk, T. K., and C. J. Shiff. 2000. Recovery of avian schistosome cercariae from water using penetration stimulant matrix with an unsaturated fatty acid. American Journal of Tropical Medicine and Hygiene 63:174–177. https://doi.org/10.4269/ajtmh.2000.63.174.

Johnson, P. T. J., J. R. Rohr, J. T. Hoverman, E. Kellermanns, J. Bowerman, and K. B. Lunde. 2012. Living fast and dying of infection: host life history drives interspecific variation in infection and disease risk. Ecology Letters 15:235–242. https://doi.org/10.1111/j.1461-0248.2011.01730.x.

Johnson, P. T. J., D. R. Sutherland, J. M. Kinsella, and K. B. Lunde. 2004. Review of the trematode genus *Ribeiroia* (Psilostomidae): ecology, life history and pathogenesis with special emphasis on the amphibian malformation problem. Advances in Parasitology 57:191–253. https://doi.org/10.1016/S0065-308X(04)57003-3.

Kirk, D., N. Jones, S. Peacock, J. Phillips, P. K. Molnár, M. Krkosek, and P. Luijckx. 2018. Empirical evidence that metabolic theory describes the temperature dependency of within-host parasite dynamics. PLoS Biology 16:e2004608. https://doi.org/10.1371/journal.pbio.2004608.

LaFonte, B. E., and P. T. J. Johnson. 2013. Experimental infection dynamics: using immunosuppression and in vivo parasite tracking to understand host resistance in an amphibian-trematode system. Journal of Experimental Biology 216:3700–3708. https://doi.org/10.1242/jeb.088104.

Luhring, T. M., and J. P. DeLong. 2016. Predation changes the shape of thermal performance curves for population growth rate. Current Zoology 62:501–505. https://doi.org/10.1093/cz/zow045.

Mangoni, M. L., R. Miele, T. G. Renda, D. Barra, and M. Simmaco. 2001. The synthesis of antimicrobial peptides in the skin of *Rana esclenta* is stimulated by microorganisms. FASEB Journal 15:1431–1432. https://doi.org/10.1096/fj.00–0695fje.

McWhinnie, R. B., J. P. Sckrabulis, and T. R. Raffel. 2021. Temperature and mass scaling affect cutaneous and pulmonary respiratory performance in a diving frog. Integrative Zoology 16:712–728. https://doi.org/10.1111/1749-4877.12551.

Molnár, P. K., S. J. Kutz, B. M. Hoar, and A. P. Dobson. 2013. Metabolic approaches to understanding climate change impacts on seasonal host-macroparasite dynamics. Ecology Letters 16:9–21. https://doi.org/10.1111/ele.12022.

Molnár, P. K., J. P. Sckrabulis, K. A. Altman, and T. R. Raffel. 2017. Thermal performance curves and the metabolic theory of ecology—a practical guide to models and experiments for parasitologists. Journal of Parasitology 103:423–439. https://doi.org/10.1645/16-148.

Narum, S. R., N. R. Campbell, K. A. Meyer, M. R. Miller, and R. W. Hardy. 2013. Thermal adaptation and acclimation of ectotherms from differing aquatic climates. Molecular Ecology 22:3090–3097. https://doi.org/10.1111/mec.12240.

Öhlund, G., P. Hedström, S. Norman, C. L. Hein, and G. Englund. 2015. Temperature dependence of predation depends on the relative performance of predators and prey. Proceedings of the Royal Society B 282:20142254. https://doi.org/10.1098/rspb.2014.2254.

Patel, N., T. Kreider, J. F. Urban, and W. C. Gause. 2009. Characterisation of effector mechanisms at the host-parasite interface during the immune response to tissue-dwelling intestinal nematode parasites. International Journal for Parasitology 39:13–21. https://doi.org/10.1016/j.ijpara.2008.08.003.

Paull, S. H., T. R. Raffel, B. E. LaFonte, and P. T. J. Johnson. 2015. How temperature shifts affect parasite production: testing the roles of thermal stress and acclimation. Functional Ecology 29:941–950. https://doi.org/10.1111/1365-2435.12401.

Pochini, K. M., and J. T. Hoverman. 2017. Intermediate and lag effects of pesticide exposure on parasite resistance in larval

amphibians. Parasitology 144:817–822. https://doi.org/10.1017/S0031182016002560.

R Core Team. 2020. R: a language and environment for statistical computing. R Foundation for Statistical Computing, Vienna.

Raffel, T. R., J. M. Romansic, N. T. Halstead, T. A. MacMahon, M. D. Venesky, and J. R. Rohr. 2013. Disease and thermal acclimation in a more variable and unpredictable climate. Nature Climate Change 3:146–151. https://doi.org/10.1038/nclimate1659.

Régnière, J., and J. Powell. 2003. Animal life cycle models. Pages 295–315 *in* Phenology: an integrative environmental science. M. D. Schwaz, ed. Springer, Berlin.

Régnière, J., J. Powell, B. Bentz, and V. Nealis. 2012. Effects of temperature on development, survival and reproduction of insects: experimental design, data analysis and modeling. Journal of Insect Physiology 58:634–647. https://doi.org/10.1016/j.jinsphys.2012.01.010.

Rohr, J. R., D. J. Civitello, J. M. Cohen, E. A. Roznik, B. Sinervo, and A. I. Dell. 2018. The complex drivers of thermal acclimation and breadth in ectotherms. Ecology Letters 21:1425–1439. https://doi.org/10.1111/ele.13107.

Rohr, J. R., and J. M. Cohen. 2020. Understanding how temperature shifts could impact infectious disease. PLoS Biology 18: e3000098. https://doi.org/10.1371/journal.pbio.3000938.

Rohr, J. R., T. R. Raffel, A. R. Blaustein, P. T. J. Johnson, S. H. Paull, and S. Young. 2013. Using physiology to understand climate-driven changes in disease and their implication for conservation. Conservation Physiology 1:cot022. https://doi.org/10.1093/conphys/cot022.

Rohr, J. R., T. R. Raffel, S. K. Sessions, and P. J. Hudson. 2008. Understanding the net effects of pesticides on amphibian trematode infections. Ecological Applications 18:1743–1753. https://doi.org/10.1890/07-1429.1.

Rollins-Smith, L. A., J. K. Doersam, J. E. Longcore, S. K. Taylor, J. C. Shamblin, C. Carey, and M. A. Zasloff. 2002. Antimicrobial peptide defenses against pathogens associated with global amphibian declines. Developmental and Comparative Immunology 26:63–72. https://doi.org/10.1016/S0145-305X(01)00041-6.

Schoolfield, R. M., P. J. H. Sharpe, and C. E. Magnuson. 1981. Non-linear regression of biological temperature-dependent rate models based on absolute reaction-rate theory. Journal of Theoretical Biology 88:719–731. https://doi.org/10.1016/0022-5193(81)90246-0.

Sckrabulis, J. P., K. A. Altman, and T. R. Raffel. 2022. Data from: Using metabolic theory to describe temperature and thermal acclimation effects on parasitic infection. American Naturalist, Dryad Digital Repository, https://doi.org/10.5061/dryad.bnzs7h4c7.

Shi, P., and F. Ge. 2010. A comparison of different thermal performance functions describing temperature-dependent development rates. Journal of Thermal Biology 35:225–231. https://doi.org/10.1016/j.jtherbio.2010.05.005.

Smith, N. F., and J. H. Cohen. 2012. Comparative photobehavior of marine cercariae with differing secondary host preferences. Biological Bulletin 222:74–83. https://doi.org/10.1086/BBLv222n1p74.

Studer, A., and R. Poulin. 2013. Differential effects of temperature variability on the transmission of a marine parasite. Marine Biology 160:2763–2773. https://doi.org/10.1007/s00227-013-2269-6.

Szuroczki, D., and J. M. L. Richardson. 2012. The behavioral response of larval amphibians (Ranidae) to threats from predators and parasites. PLoS ONE 7:e49592. https://doi.org/10.1371/journal.pone.0049592.

Taylor, C. N., K. L. Oseen, and R. J. Wassersug. 2004. On the behavioural response of *Rana* and *Bufo* tadpoles to echinostomatoid cercariae: implications to synergistic factors influencing trematode infections in anurans. Canadian Journal of Zoology 82:701–706. https://doi.org/10.1139/Z04-037.

Thomas, M. B., and S. Blanford. 2003. Thermal biology in insect-parasite interactions. Trends in Ecology and Evolution 18:344–350. https://doi.org/10.1016/S0169-5347(03)00069-7.

Tomanek, L., and G. N. Somero. 1999. Evolutionary and acclimation-induced variation in the heat-shock responses of congeneric marine snails (genus: *Tegula*) from different thermal habitats: implications for limits of thermotolerance and biogeography. Journal of Experimental Biology 202:2925–2936.

Wilson, R. S., and C. E. Franklin. 2002. Testing the beneficial acclimation hypothesis. Trends in Ecology and Evolution 17:66–70. https://doi.org/10.1016/S0169-5347(01)02384-9.

Wilson, R. S., R. S. James, and I. A. Johnston. 2000. Thermal acclimation of locomotor performance in tadpoles and adults of the aquatic frog *Xenopus laevis*. Journal of Comparative Physiology B 170:117–124.

Woodhams, D. C., L. A. Rollins-Smith, R. A. Alford, M. A. Simon, and R. N. Harris. 2007. Innate immune defenses of amphibian skin: antimicrobial peptides and more. Animal Conservation 10:425–428. https://doi.org/10.1111/j.1469-1795.2007.00150.x.

Xiao, X., E. P. White, M. B. Hooten, and S. L. Durham. 2011. On the use of log-transformation vs. nonlinear regression for analyzing biological power laws. Ecology 92:1887–1894. https://doi.org/10.1890/11-0538.1.

References Cited Only in the Online Enhancements

Cohen, L. M., H. Neimark, and L. K. Eveland. 1980. *Schistosoma mansoni*: response of cercariae to a thermal gradient. Journal of Parasitology 66:362–364. https://doi.org/10.2307/3280843.

Gosner, K. L. 1960. A simplified table for staging anuran embryos and larvae with notes on identification. Herpetologica 16:183–190.

Johnson, P. T. J., J. M. Chase, K. L. Dosch, R. B. Hartson, J. A. Gross, D. J. Larson, D. R. Sutherland, and S. R. Carpenter. 2007. Aquatic eutrophication promotes pathogenic infection in amphibians. Proceedings of the National Academy of Sciences of the USA 104:15781–15786. https://doi.org/10.1073/pnas.0707763104.

Nussbaum-Krammer, C. I., M. F. Neto, R. M. Brielmann, J. S. Pederson, and R. I. Morimoto. 2015. Investigating the spreading and toxicity of prion-like proteins using the metazoan model organism *C. elegans*. Journal of Visualized Experiments 95:e52321. https://doi.org/10.3791/52321.

Padfield, D., and G. Matheson. 2018. Nls.multstart: an R package for robust non-linear regression using AIC scores. v1.0.0.

Associate Editor: Benjamin Gilbert
Editor: Daniel I. Bolnick